

Functional renormalization group for non-equilibrium quantum many-body problems

R. Gezzi, Th. Pruschke, and V. Meden

*Institut für Theoretische Physik, Universität Göttingen,
Friedrich-Hund-Platz 1, D-37077 Göttingen, Germany*

(Dated: November 5, 2019)

We extend the concept of the functional renormalization for quantum many-body problems to non-equilibrium situations. Using a suitable generating functional based on the Keldysh approach, we derive a system of coupled differential equations for the m -particle vertex functions. The approach is completely general and allows calculations for both stationary and time-dependent situations. As a specific example we study the stationary state transport through a quantum dot with local Coulomb correlations at finite bias voltage employing two different truncation schemes for the infinite hierarchy of equations arising in the functional renormalization group scheme.

PACS numbers: 71.27.+a,73.21.La,73.23.-b

I. INTRODUCTION

The reliable calculation of physical properties of interacting quantum mechanical systems presents a formidable task. Typically, one has to cope with the interplay of different energy-scales possibly covering several orders of magnitude even for simple situations. Approximate tools like perturbation theory, but even numerically exact techniques can usually handle only a restricted window of energy scales and are furthermore limited in their applicability by the approximations involved or the computational resources available. In addition, due to the divergence of certain classes of Feynman diagrams, some of the interesting many-particle problems cannot be tackled by straight forward perturbation theory.

The situation becomes even more involved if one is interested in properties off equilibrium, in particular time-dependent situations. A standard approach for such cases is based on the Keldysh formalism¹ for the time evolution of Green functions, resulting in a matrix structure of propagators and self-energies. This structure is a direct consequence of the fact that in non-equilibrium we have to calculate averages of operators taken not with respect to the ground state but with respect to an arbitrary state. Therefore, the Gell-Mann and Low theorem² is not valid any more. Other approaches attempt to treat the time evolution of the non-equilibrium system numerically, for example using the density matrix renormalization group³ or the numerical renormalization group (NRG)^{4,5} or flow-equations.⁶

Despite its more complicated structure the Keldysh technique shows a big flexibility and one therefore can find a wide range of applications such as transport through atomic, molecular and nano devices under various conditions,⁷ systems of atoms interacting with a radiation field in contact with a bath,^{8,9} or electron-electron interaction in a weakly ionized plasma.¹⁰

One powerful concept to study interacting many-particle systems is the rather general idea of the renormalization group¹¹ (RG), which has also been applied to time-dependent and stationary non-equilibrium situations recently.^{12,13,14,15} In the RG approach one starts

from high energy scales, leaving out possible infrared divergences and works ones way down to the desired low-energy region in a systematic way. However, the precise definition of “systematic way” does in general depend on the problem studied.

In order to resolve this ambiguity, in particular for interacting quantum mechanical many-particle systems in equilibrium, two different schemes attempting a unique, problem independent prescription have emerged during the past decade. One is Wegner’s Hamiltonian based flow-equation technique,^{16,17} the second a field theoretical approach, which we want to focus on in the following. This approach is based on a functional representation of the partition function of the system and has become known as functional renormalization group (FRG).^{18,19,20,21}

A detailed description of the various possible implementations of the FRG and its previous applications can be found e.g. in Refs. 22,23. In the present work we formally extend the FRG to non-equilibrium by formulating the problem on the real instead of the imaginary time axis using the functional integral representation of the action on the Keldysh contour. Within a diagrammatic approach a similar set of FRG flow equations has already been derived by Jakobs and Schoeller and applied to study non-linear transport through one-dimensional correlated electron systems.^{24,25} We believe that this method will enable us to treat a variety of non-equilibrium problems within a scheme which is well established in equilibrium and in contrast to other approaches is comparatively modest with respect to the computer resources required. Our framework for non-equilibrium will turn out to be sufficiently general to allow for a treatment of systems disturbed by arbitrary external fields (bias voltage, laser field, etc.), which can be constant or time-dependent. For classical many-body problems the FRG (also called non-perturbative renormalization group) was generalized to non-equilibrium to study transitions between stationary states.²⁶

As a simple but non-trivial application to test the potential and weakness of our implementation of a non-equilibrium FRG we choose the single impurity Anderson

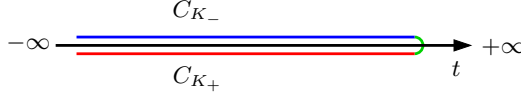


FIG. 1: (color online) Keldysh contour

model (SIAM).²⁷ This model represents the paradigm for correlation effects in condensed matter physics and is at the heart of a large range of experimental^{28,29,30,31,32,33,34} and theoretical investigations.^{35,36}

The paper is organized as follows. In the next section and the appendices we discuss the formal extension of the FRG to general non-equilibrium situations. In order to test the method, we discuss its application to the stationary transport through an Anderson impurity, the standard model for the description of the transport properties of interacting quantum dots, at $T = 0$ in section III. Within the non-equilibrium extension we obtain a system of coupled tensor equations, which represent the flow of the different components (in the Keldysh space) of the self-energy and the vertex function. We discuss two approximations derived from the FRG scheme that have been successfully applied to the equilibrium situation before.^{37,38} A summary and discussion with outlook in section IV concludes the paper.

II. FRG IN NON-EQUILIBRIUM

We start from the standard definition of the two-time Green function

$$G(1, 2) = -i \langle S^{-1} [T\psi_H(1)\psi_H^\dagger(2)] S \rangle , \quad (1)$$

in the interaction picture, where the labels “1” and “2” comprise a set of quantum numbers and time. The time evolution operators are given as

$$S = T \exp \left\{ -i \int_{-\infty}^{\infty} V_I(t) dt \right\} \quad (2)$$

$$S^{-1} = \tilde{T} \exp \left\{ i \int_{+\infty}^{-\infty} V_I(t) dt \right\} , \quad (3)$$

with T the usual time ordering and \tilde{T} the anti time-ordering operator. The interaction term $V_I(t)$ is arbitrary up to now, including possible explicit time dependence.

In a non-equilibrium situation, the propagation of the system from $-\infty \rightarrow \infty$ is not any more equivalent to the propagation from $\infty \rightarrow -\infty$, i.e. one has to distinguish whether the time arguments in (1) belong to the former or latter.^{39,40,41} This scheme is usually depicted by the

double-time contour shown in Fig. 1, where C_{K_-} represents the propagation $-\infty \rightarrow +\infty$ and C_{K_+} the propagation $+\infty \rightarrow -\infty$. Consequently, one has to introduce four distinct propagators, namely the time-ordered Green function

$$\begin{aligned} G^{--}(1, 2) &= -i \langle T\psi(1)\psi^\dagger(2) \rangle \\ &= -i\theta(t_1 - t_2) \langle \psi(1)\psi^\dagger(2) \rangle - \zeta i\theta(t_2 - t_1) \langle \psi^\dagger(2)\psi(1) \rangle \end{aligned} \quad (4)$$

where $t_1, t_2 \in C_{K_-}$, the anti time-ordered Green function

$$\begin{aligned} G^{++}(1, 2) &= -i \langle \tilde{T}\psi(1)\psi^\dagger(2) \rangle \\ &= -i\theta(t_2 - t_1) \langle \psi(1)\psi^\dagger(2) \rangle - \zeta i\theta(t_1 - t_2) \langle \psi^\dagger(2)\psi(1) \rangle \end{aligned} \quad (5)$$

with $t_1, t_2 \in C_{K_+}$ and

$$G^{+-}(1, 2) = -i \langle \psi(1)\psi^\dagger(2) \rangle , t_1 \in C_{K_+}, t_2 \in C_{K_-} \quad (6)$$

$$G^{-+}(1, 2) = -\zeta i \langle \psi^\dagger(2)\psi(1) \rangle , t_1 \in C_{K_-}, t_2 \in C_{K_+} \quad (7)$$

where $\zeta = +1$ for bosons and $\zeta = -1$ for fermions. $G^{--}(1, 2)$ and $G^{++}(1, 2)$ take into account the excitation spectrum while $G^{+-}(1, 2)$ and $G^{-+}(1, 2)$ describe the thermodynamic state of the system. Note that not all of them are independent, but one can in fact introduce linear combinations, the best known of which are

$$G^R(t, t') := \theta(t - t') [G^{+-}(t, t') + \zeta G^{-+}(t, t')] \quad (8)$$

$$G^A(t, t') := \theta(t' - t) [G^{+-}(t, t') + \zeta G^{-+}(t, t')] \quad (9)$$

$$G^K(t, t') := G^{-+}(t, t') + G^{+-}(t, t') , \quad (10)$$

named retarded, advanced and Keldysh component, respectively.

To derive a FRG scheme along the lines given in 22,23 one needs a formulation that allows to express the m -particle vertices as functional derivatives of a generating functional. Here we use the approach by Kameneev.⁴² To this end we define the matrix

$$\hat{G} := \begin{pmatrix} G^{--} & G^{-+} \\ G^{+-} & G^{++} \end{pmatrix}$$

and the short hand notation

$$(\bar{\psi}, \hat{O}\psi) := i \int_{-\infty}^{\infty} d\xi d\xi' \bar{\psi}(\xi) \hat{O}(\xi, \xi') \psi(\xi') ,$$

where

$$\psi = \begin{pmatrix} \psi_- \\ \psi_+ \end{pmatrix}$$

is the vector of the fields (Grassmann for fermions or complex for bosons) and ξ a collection of all quantum numbers and time. The generalization of the partition function is⁴²

$$\Xi = \frac{1}{\Xi_0} \int \mathcal{D}\bar{\psi}\psi \exp \left\{ \left(\bar{\psi}, \left[\hat{G}_0 \right]^{-1} \psi \right) - iS_{\text{int}}(\{\bar{\psi}\}, \{\psi\}) \right\}, \quad \Xi_0 = \int \mathcal{D}\bar{\psi}\psi \exp \left\{ \left(\bar{\psi}, \left[\hat{G}_0 \right]^{-1} \psi \right) \right\}. \quad (11)$$

The matrix \hat{G}_0 denotes the propagator of a suitable chosen non-interacting reference system and S_{int} is the (arbitrary) interaction term.

To construct a generating functional for m -particle Green functions, one introduces external source fields η and $\bar{\eta}$ according to

$$\mathcal{W}(\{\bar{\eta}\}, \{\eta\}) = \frac{1}{\Xi_0} \int \mathcal{D}\bar{\psi}\psi \exp \left\{ \left(\bar{\psi}, \left[\hat{G}_0 \right]^{-1} \psi \right) - iS_{\text{int}}(\{\bar{\psi}\}, \{\psi\}) - (\bar{\psi}, \eta) - (\bar{\eta}, \psi) \right\}, \quad (12)$$

The (connected) m -particle Green function $G_m^{(c)}$ can then be obtained by taking functional derivatives

$$G_m^{(c)}(\{\xi'_j\}; \{\xi_j\}) = (\zeta i)^m \frac{\delta^m}{\delta \bar{\eta}_{\xi'_1} \dots \delta \bar{\eta}_{\xi'_m}} \frac{\delta^m}{\delta \eta_{\xi_m} \dots \delta \eta_{\xi_1}} \mathcal{W}^{(c)}(\{\bar{\eta}\}, \{\eta\}) \Big|_{\eta=\bar{\eta}=0} \quad (13)$$

with

$$\mathcal{W}^c(\{\bar{\eta}\}, \{\eta\}) = \ln [\mathcal{W}(\{\bar{\eta}\}, \{\eta\})]. \quad (14)$$

Note that the derivatives in (13) are taken with respect to the spinors η , i.e. the resulting quantity $G_m^{(c)}$ is a tensor of rank $2m$ in the Keldysh indices. In the following we adopt the notation that quantities with explicit index m are tensors of rank $2m$; without index m we denote the one-particle Green function and self-energy, both carrying a hat to point out their matrix structure.

Introducing the fields

$$\phi_\xi = i \frac{\delta}{\delta \bar{\eta}_\xi} \mathcal{W}^c(\{\bar{\eta}\}, \{\eta\})$$

we can perform a Legendre transformation

$$\begin{aligned} \Gamma(\{\bar{\phi}\}, \{\phi\}) &= -\mathcal{W}^c(\{\bar{\eta}\}, \{\eta\}) - i(\bar{\phi}, \eta) - i(\bar{\eta}, \phi) \\ &+ i \left(\bar{\phi}, \left[\hat{G}_0 \right]^{-1} \phi \right), \end{aligned} \quad (16)$$

to the generating functional of the one-particle irreducible vertex functions γ_m

$$\gamma_m(\{\xi'_j\}; \{\xi_j\}) = i^m \frac{\delta^m}{\delta \bar{\phi}_{\xi'_1} \dots \delta \bar{\phi}_{\xi'_m}} \frac{\delta^m}{\delta \phi_{\xi_m} \dots \delta \phi_{\xi_1}} \Gamma(\{\bar{\phi}\}, \{\phi\}) \Big|_{\phi=\bar{\phi}=0}. \quad (17)$$

Note that in contrast to the usual definition⁴³ of Γ for convenience (see below) we have added a term $\left(\bar{\phi}, \left[\hat{G}_0 \right]^{-1} \phi \right)$ in Eq. (16). The relation between the

$G_m^{(c)}$ and γ_m can be found in standard text books.⁴³ For example, for the one-particle Green function we obtain

$$\begin{aligned} G_1(\xi'; \xi) &= G_1^c(\xi'; \xi) \\ &= i \frac{\delta}{\delta \bar{\eta}_{\xi'_1}} \frac{\delta}{\delta \eta_{\xi_1}} \mathcal{W}^c = -\zeta \hat{G}_{\xi', \xi}, \end{aligned}$$

$$= \left[\gamma_1 - \zeta \left[\hat{G}_0 \right]^{-1} \right]_{\xi', \xi}^{-1}$$

where

$$\hat{G}_{\xi', \xi} = \left(\left[\hat{G}_0 \right]^{-1} - \hat{\Sigma} \right)_{\xi', \xi}^{-1},$$

with the proper one particle self-energy $\hat{\Sigma}$. This implies the relation $\hat{\Sigma} = \zeta \gamma_1$. Note that we have a matrix structure not only with respect to ξ and ξ' , but also with

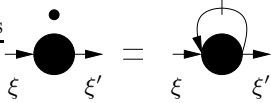


FIG. 2: Diagrammatic form of the flow equation for γ_1^A . The slashed line stands for the single scale propagator \hat{S}^A .

respect to the Keldysh indices. How does this additional structure manifests itself in the Green functions (13)? For $m = 1$ we have two derivatives with respect to vector fields, i.e. the structure of a tensor product, which can be made explicit by using a tensor product notation

$$G_1^c(\xi', \xi) = (\zeta i) \frac{\delta}{\delta \bar{\eta} \xi'} \otimes \frac{\delta}{\delta \eta \xi} \mathcal{W}^c \Big|_{\eta = \bar{\eta} = 0} ,$$

leading to the matrix

$$\begin{aligned} G_1^c(\xi', \xi) &= (\zeta i) \begin{pmatrix} \frac{\delta^2 \mathcal{W}^c}{\delta \bar{\eta}_-(\xi') \delta \eta_-(\xi)} & \frac{\delta^2 \mathcal{W}^c}{\delta \bar{\eta}_-(\xi') \delta \eta_+(\xi)} \\ \frac{\delta^2 \mathcal{W}^c}{\delta \bar{\eta}_+(\xi') \delta \eta_-(\xi)} & \frac{\delta^2 \mathcal{W}^c}{\delta \bar{\eta}_+(\xi') \delta \eta_+(\xi)} \end{pmatrix} \\ &= \begin{pmatrix} G^{--}(\xi', \xi) & G^{-+}(\xi', \xi) \\ G^{+-}(\xi', \xi) & G^{++}(\xi', \xi) \end{pmatrix} . \end{aligned} \quad (18)$$

Thus the Keldysh structure enters into the equations by a simple extension of the index space $(\pm, \xi) \rightarrow \xi$.

Up to now we performed standard text book manipulations. We emphasize once more that our functionals are formulated in *real time* and no translational invariance in time is assumed. The derivation of the actual FRG equations is now completely analogous to Ref. 23. In Eqs. (11) and (12) we replace the non-interacting propagator by a propagator \hat{G}_0^Λ depending on some parameter $\Lambda \in [\Lambda_0, 0]$ and require

$$\hat{G}_0^{\Lambda_0} = 0 , \quad \hat{G}_0^{\Lambda=0} = \hat{G}_0 , \quad (19)$$

i.e. at the starting point $\Lambda = \Lambda_0$ no degrees of freedom are “turned on” while at $\Lambda = 0$ the cutoff free problem is recovered. Through \hat{G}_0^Λ the quantities defined in Eqs. (11) to (17) acquire a Λ -dependence. One now derives a functional differential equation for Γ^Λ . From this, by expanding in powers of the external sources, an infinite hierarchy of coupled differential equations for the γ_m^Λ is obtained. Although the steps in the derivation are, as already emphasized, formally equivalent to Ref. 23, because of the real-time formulation additional factors i and signs appear in several places. We thus believe that it is helpful to present the details of the derivation for the present approach, which is done in Appendix A.

In particular, for the flow of the self-energy one finds the expression

$$\begin{aligned} \frac{d}{d\Lambda} \gamma_1^\Lambda(\xi'; \xi) &= \zeta \frac{d}{d\Lambda} \hat{\Sigma}^\Lambda(\xi', \xi) \\ &= \text{Tr} \left[\hat{S}^\Lambda \gamma_2^\Lambda(\xi', \cdot; \xi, \cdot) \right] , \end{aligned} \quad (20)$$

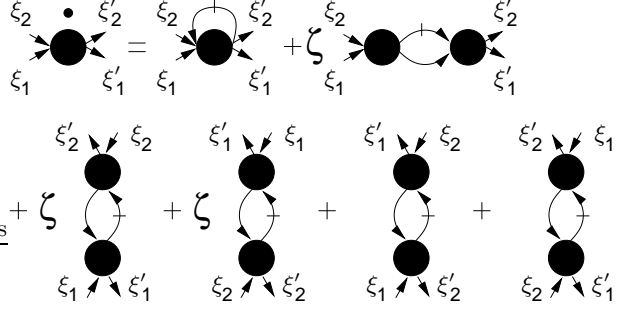


FIG. 3: Diagrammatic form of the flow equation for γ_2^Λ . The slashed line stands for the single scale propagator \hat{S}^Λ , the unslashed line for \hat{G}^Λ .

which can be visualized by the diagram in Fig. 2. The trace in (20) is meant to run over all internal quantum numbers and time respectively frequency. In (20) appears the so-called single scale propagator (the slashed line in Fig. 2)

$$\hat{S}^\Lambda = \hat{G}^\Lambda \hat{Q}^\Lambda \hat{G}^\Lambda , \quad (21)$$

$$\hat{Q}^\Lambda = \frac{d}{d\Lambda} \left[\hat{G}_0^\Lambda \right]^{-1} . \quad (22)$$

and the quantity $\gamma_2^\Lambda(\xi', \cdot; \xi, \cdot)$ denotes the matrix obtained by keeping the indices ξ and ξ' fixed.

We thus arrive at an expression that is formally identical to Eq. (19) in Ref. 23. The difference appears in the matrix structure, which now also contains the index components for the branches of the Keldysh contour. To make this explicit, we write out Eq. (20) with respect to the Keldysh structure

$$\zeta \frac{d}{d\Lambda} \Sigma^{\alpha\beta,\Lambda}(\xi', \xi) = \text{Tr} \sum_{\mu\nu} \mathcal{S}^{\mu\nu,\Lambda} \gamma_2^{\alpha\nu;\beta\mu,\Lambda}(\xi', \cdot; \xi, \cdot) . \quad (23)$$

Apparently, the derivative of γ_1^Λ is determined by γ_1^Λ and the two-particle vertex γ_2^Λ . Thus an equation for γ_2^Λ is required. The structure of this equation again turns out to be identical to Eq. (21) in Ref. 23. Here we only show the diagrams representing it in Fig. 3, the full expression can be found in Appendix B. The differential equation for γ_2^Λ does not only contain γ_1^Λ – implicitly via the propagators – and γ_2^Λ , but also the three-particle vertex γ_3^Λ . The flow of the three-particle vertex depends on the four-particle vertex etc. It is generically impossible to solve the full set of infinitely many coupled differential equations. In applications one has to truncate it, and this is usually done at $m = 2$, i.e. one replaces all vertices with $m > 2$ by their initial values, which for problems containing a two-particle interaction means $\gamma_m = 0$ for $m > 2$. Note that even within this truncated system the remaining set of differential equations must typically still be further approximated to allow a numerical solution.^{37,38,44}

Let us note again that a similar set of flow equations was independently derived by Jakobs and Schoeller using a diagrammatic approach.^{24,25}

III. APPLICATION TO QUANTUM DOTS

The derivation of the flow equations in the previous section and the appendices was completely general and they can be used to study time dependent or stationary properties of systems at finite temperature or $T = 0$. A simple but nonetheless non-trivial application is non-equilibrium, stationary transport through an interacting quantum dot at $T = 0$. For a stationary situation, time translational invariance holds and one can Fourier transform to frequency space. Moreover, because the quantum dot is a zero-dimensional structure, no additional degrees of freedom except spin have to be taken into account, thus considerably reducing the complexity of the problem.

Non-equilibrium theory of quantum dots, or equivalently the SIAM (see below) has been a major subject of research over the past years. Several techniques have been developed respectively applied, for example statistical^{45,46,47} and perturbational treatment,^{48,49,50,51,52,53,54,55,56} RG based^{13,15} and numerical procedures.^{5,6} In particular the RG based calculations were up to now restricted to situations far away from the Kondo regime, either by looking at features in the mixed-valence state¹³ or in strong magnetic fields.¹⁵ Thus, despite a tremendous ongoing effort, relatively little is known about non-equilibrium properties, even in the stationary state, of the model. On the other hand, the very detailed knowledge of the *equilibrium* properties⁵⁷ makes it possible to interpret certain features or even dismiss approximations on the basis of this fundamental understanding.

A. Single impurity Anderson model

The standard model to describe transport through interacting quantum dots is the SIAM.²⁷ Experimentally,^{28,58} the dot region is attached to two external leads, and the current is driven by an applied bias voltage V_B . Furthermore, the filling of the dot can be controlled by a gate voltage V_G . To keep notation simple we use as unit for the charge $e = 1$ in the following. The resulting Hamiltonian then reads

$$H = \sum_{\vec{k}\sigma\alpha} \varepsilon_{\vec{k}\sigma\alpha} c_{\vec{k}\sigma\alpha}^\dagger c_{\vec{k}\sigma\alpha} + \sum_{\sigma} V_G d_{\sigma}^\dagger d_{\sigma} + U \left(n_{\uparrow} - \frac{1}{2} \right) \left(n_{\downarrow} - \frac{1}{2} \right) + \sum_{\vec{k}\sigma\alpha} \left[V_{\vec{k}\sigma\alpha} c_{\vec{k}\sigma\alpha}^\dagger d_{\sigma} + h.c. \right] \quad (24)$$

in standard second quantized notation ($n_{\sigma} = d_{\sigma}^\dagger d_{\sigma}$). As usual, \vec{k} is the wave vector of the band states in the leads and σ the spin. In addition to those two quantum numbers the index $\alpha = L, R$ distinguishes the left and right reservoirs which can have different chemical potentials μ_{α} through an applied bias voltage $V_B = \mu_L - \mu_R$. Since

we do not include a magnetic field, the spin dependence will be dropped in the following. Furthermore, we assume the dispersions $\varepsilon_{\vec{k}\sigma\alpha}$ and hybridizations $V_{\vec{k}\sigma\alpha}$ between dot and the left and right leads respectively to be identical, and $V_{\vec{k}} \equiv V/\sqrt{2}$ to be \vec{k} -independent. Note that (24) is written such that for $V_G = 0$ we have particle-hole symmetry.

For the flow equations we need the propagator $\hat{G}_{d,0}$ for $U = 0$. To this end we use the Dyson equation to obtain^{1,39,41}

$$\hat{G}_{d,0}(\omega) = \left[\begin{pmatrix} \omega - V_G & 0 \\ 0 & -\omega + V_G \end{pmatrix} - \hat{\Sigma}^{(0)} \right]^{-1}, \quad (25)$$

where

$$\begin{aligned} \hat{G}_{d,0} &= \begin{pmatrix} G_{d,0}^{--} & G_{d,0}^{-+} \\ G_{d,0}^{+-} & G_{d,0}^{++} \end{pmatrix}, \\ \hat{\Sigma}^{(0)} &= \frac{V^2}{2N} \sum_{\vec{k}\alpha} \begin{pmatrix} G_{\vec{k}\alpha}^{--} & G_{\vec{k}\alpha}^{-+} \\ G_{\vec{k}\alpha}^{+-} & G_{\vec{k}\alpha}^{++} \end{pmatrix}. \end{aligned} \quad (26)$$

In order to further evaluate (26), we need the Green functions of the free electron gas, given by

$$G_{\vec{k}\alpha}^{--}(\omega) = \frac{1}{\omega - \varepsilon_{\vec{k}} + \mu_{\alpha} + i\delta} \quad (27)$$

$$+ 2i\pi f(\varepsilon_{\vec{k}}) \delta(\omega - \varepsilon_{\vec{k}} + \mu_{\alpha}),$$

$$G_{\vec{k}\alpha}^{++}(\omega) = -[G_{\vec{k}\alpha}^{--}(\omega)]^*, \quad (28)$$

$$G_{\vec{k}\alpha}^{-+}(\omega) = 2i\pi f(\varepsilon_{\vec{k}}) \delta(\omega - \varepsilon_{\vec{k}} + \mu_{\alpha}), \quad (29)$$

$$G_{\vec{k}\alpha}^{+-}(\omega) = -2i\pi f(-\varepsilon_{\vec{k}}) \delta(\omega - \varepsilon_{\vec{k}} + \mu_{\alpha}). \quad (30)$$

Inserting these equations into (25) we obtain the following expressions

$$G_{d,0}^{--}(\omega) = \frac{\omega - V_G - i\Gamma [1 - f_L(\omega) - f_R(\omega)]}{(\omega - V_G)^2 + \Gamma^2}, \quad (31)$$

$$G_{d,0}^{++}(\omega) = -[G_{d,0}^{--}(\omega)]^*, \quad (32)$$

$$G_{d,0}^{-+}(\omega) = i \frac{\Gamma [f_L(\omega) + f_R(\omega)]}{(\omega - V_G)^2 + \Gamma^2}, \quad (33)$$

$$G_{d,0}^{+-}(\omega) = -i \frac{\Gamma [f_L(-\omega) + f_R(-\omega)]}{(\omega - V_G)^2 + \Gamma^2}, \quad (34)$$

where $f_{\alpha}(\pm\omega) := f(\pm(\omega - \mu_{\alpha}))$ are the Fermi functions of the leads and $\Gamma = \pi|V|^2 N_F$, with N_F the density of states at the Fermi level of the semi-infinite leads, represents the tunnel barrier between the leads and the impurity.

Finally, the quantity we eventually want to calculate is the current J through the dot or the differential conductance $G = dJ/dV_B$. For the model (24) the current is given by the formula^{7,51}

$$\begin{aligned} J &= J_L + J_R \quad (35) \\ &= \frac{ie\Gamma}{2\pi\hbar} \int d\epsilon [f_L(\epsilon) - f_R(\epsilon)] [G_d^{+-}(\epsilon) - G_d^{-+}(\epsilon)], \end{aligned}$$

where we already used that the left and right couplings are identical, i.e. $\Gamma_L = \Gamma_R = \Gamma/2$, and summed over both spin directions. Note that Eq. (35) is written in a somewhat unusual form, not employing the relation $G_d^{+-}(\epsilon) - G_d^{-+}(\epsilon) = G_d^R(\epsilon) - G_d^A(\epsilon) = -2\pi i \rho_d(\epsilon)$, where ρ_d denotes the dot's one-particle spectral function. The

reason for this will be explained below.

Another quantity of interest is $\Delta J := J_L - J_R$.⁴⁹ Obviously, since no charge is produced on the quantum dot, $\Delta J = 0$ in the exact solution. Using again the results of 7,51, the expression for ΔJ becomes

$$\Delta J = -\frac{e\Gamma}{\pi\hbar} \int_{-\infty}^{\infty} d\omega \frac{F(\omega) [\Im m\Sigma^{+-}(\omega) - \Im m\Sigma^{+-}(-\omega)] - 2\Im m\Sigma^{+-}(\omega)}{\tilde{\Delta}(\omega)} \quad (36)$$

$$\begin{aligned} \tilde{\Delta}(\omega) &:= |\omega - V_G + i\Gamma [1 - F(\omega)] - \Sigma^{--}(\omega)|^2 + [\Gamma F(-\omega) + \Im m\Sigma^{+-}(\omega)] [\Gamma F(\omega) - \Im m\Sigma^{+-}(\omega)] \\ F(\omega) &:= f_L(\omega) + f_R(\omega) \end{aligned} \quad (37)$$

where we used that $\Sigma^{+-}(\omega)$ and $\Sigma^{+-}(\omega)$ are purely imaginary. Depending on the type of approximation used $\Delta J = 0$ might either hold for all parameters^{51,56} or not.⁴⁹ We note that fulfilling $\Delta J = 0$ is, however, not sufficient for an approximation to provide reliable results.

B. The lowest order approximation

Before studying the coupled system $\dot{\hat{\Sigma}}, \dot{\gamma}_2$ we begin with a simpler case where we neglect $\dot{\gamma}_2$ and consider

only the flow for $\dot{\hat{\Sigma}}$. This approximation leads to at least qualitatively good results in equilibrium,³⁷ and has the additional advantage that it can be solved analytically.

Neglecting the flow of γ_2 , one has to substitute on the right hand side of (23) the initial value for γ_2 at $\Lambda = \Lambda_0$. At this point it is important to note that by virtue of Eq. (17) the vertex function has to fulfill $\gamma_2(1', 2'; 1, 2) = -\gamma_2(2', 1'; 1, 2)$ for Grassmann fields, i.e. the initial value here reads³⁹

$$\gamma_2^\Lambda(1', 2'; 1, 2) \mapsto \gamma_2^{\Lambda_0}(1', 2'; 1, 2) = (\delta_{\sigma_1, \sigma'_1} \delta_{\sigma_2, \sigma'_2} - \delta_{\sigma_1, \sigma'_2} \delta_{\sigma_2, \sigma'_1}) \begin{bmatrix} \begin{pmatrix} -iU & 0 \\ 0 & 0 \end{pmatrix} & \hat{0} \\ \hat{0} & \begin{pmatrix} 0 & 0 \\ 0 & iU \end{pmatrix} \end{bmatrix} \delta_{\sigma_1, -\sigma_2} . \quad (38)$$

With this replacement the expression (23) reduces to

$$\frac{d}{d\Lambda} \Sigma^{\mp\mp, \Lambda} = \mp iU \text{Tr} [\mathcal{S}^{\mp\mp, \Lambda}] . \quad (39)$$

Note that within this approximation the self-energy is always time (or frequency) independent, and no terms off-diagonal in the Keldysh contour indices are generated.

As last step we have to specify how the cutoff parameter Λ is introduced. Since we are interested in a stationary situation here, i.e. the propagators only depend on the time difference $t - t'$, all equations can be transformed into frequency space and one natural choice is a

frequency cutoff of the form

$$\hat{G}_{d,0}^\Lambda = \Theta(|\omega| - \Lambda) \hat{G}_{d,0} \quad (40)$$

with $\Lambda_0 \rightarrow \infty$.²³ Evaluating the factors $\hat{\mathcal{S}}$ by means of the Morris lemma^{20,23} results in

$$\hat{\mathcal{S}}^\Lambda(\omega) \rightarrow \delta(|\omega| - \Lambda) \frac{1}{\hat{G}_{d,0}(\omega)^{-1} - \hat{\Sigma}^\Lambda(\omega)} . \quad (41)$$

A straightforward calculation permits us thus to rewrite (39) as

$$\frac{d}{d\Lambda} \Sigma^{\mp\mp, \Lambda} = \pm \frac{iU}{2\pi} \sum_{\alpha=\pm 1} \frac{\frac{G_{d,0}^{\mp\mp}(\alpha\Lambda)}{\Delta(\alpha\Lambda)} - \Sigma^{\pm\pm, \Lambda}}{\left(\frac{G_{d,0}^{++}(\alpha\Lambda)}{\Delta(\alpha\Lambda)} - \Sigma^{--, \Lambda} \right) \left(\frac{G_{d,0}^{--}(\alpha\Lambda)}{\Delta(\alpha\Lambda)} - \Sigma^{++, \Lambda} \right) - \left(\frac{G_{d,0}^{++}(\alpha\Lambda)G_{d,0}^{--}(\alpha\Lambda)}{\Delta(\alpha\Lambda)^2} \right)}, \quad (42)$$

where

$$\begin{aligned} \Delta(\omega) &= G_{d,0}^{--}(\omega)G_{d,0}^{++}(\omega) - G_{d,0}^{++}(\omega)G_{d,0}^{--}(\omega) \\ &= -\frac{1}{(\omega - V_G)^2 + \Gamma^2}. \end{aligned}$$

Finally, the initial condition for the self-energy is $\lim_{\Lambda_0 \rightarrow \infty} \Sigma^{\Lambda_0} = 0$.²³

a. *Equilibrium.* We now specialize to $T = 0$ and equilibrium, i.e. $V_B = \mu_L - \mu_R = 0$. Then we obtain the decoupled system

$$\frac{d}{d\Lambda} \Sigma^{\mp\mp, \Lambda} = i \frac{U}{\pi} \frac{V_G \pm \Sigma^{\mp\mp, \Lambda}}{[(\Lambda \pm i\Gamma)^2 - (V_G \pm \Sigma^{\mp\mp, \Lambda})^2]}, \quad (43)$$

which can be solved analytically. To this end we first note that with $\Sigma^{++} = -[\Sigma^{--}]^*$ both equations are equivalent. For Σ^{--} we then obtain with the definition $\sigma := V_G + \Sigma^{--}$ as solution

$$\frac{i\sigma J_1(\frac{\pi\sigma}{U}) - (\Lambda + i\Gamma)J_0(\frac{\pi\sigma}{U})}{i\sigma Y_1(\frac{\pi\sigma}{U}) - (\Lambda + i\Gamma)Y_0(\frac{\pi\sigma}{U})} = \frac{J_0(\frac{\pi V_G}{U})}{Y_0(\frac{\pi V_G}{U})}, \quad (44)$$

where J_n Y_n are the Bessel functions of first and second kind. The desired solution of the cutoff free problem is obtained by setting $\Lambda = 0$, i.e.

$$\frac{\sigma J_1(\frac{\pi\sigma}{U}) - \Gamma J_0(\frac{\pi\sigma}{U})}{\sigma Y_1(\frac{\pi\sigma}{U}) - \Gamma Y_0(\frac{\pi\sigma}{U})} = \frac{J_0(\frac{\pi V_G}{U})}{Y_0(\frac{\pi V_G}{U})}. \quad (45)$$

which is precisely the result Eq. (4) obtained by Andergassen et al.³⁷ It is, however, important to note that in this work, based on the imaginary-time formulation of the FRG, the differential equation has a different structure. It is real and has a positive definite denominator. Thus, while the solutions at $\Lambda = 0$ are identical for the imaginary-time and real-time formulations, the flow towards $\Lambda = 0$ will show differences. As we will see next, the complex nature of the differential equation (43) can lead to problems connected to its analytical structure when attempting a numerical solution. For small U/Γ no particular problems arise. As an example the result for the flow of $\Sigma^{--, \Lambda}$ as function of Λ for $U/\Gamma = 1$ and $V_G/\Gamma = 0.5$ obtained with a standard Runge-Kutta solver is shown in Fig. 4. Consistent with the analytical solution (45), the imaginary part (dashed line) goes to zero as $\Lambda \rightarrow 0$, while the real part (solid line) rapidly approaches the value given by formula (45).

However, for larger values of U/Γ the numerical solution becomes instable in a certain regime of V_G . A typical

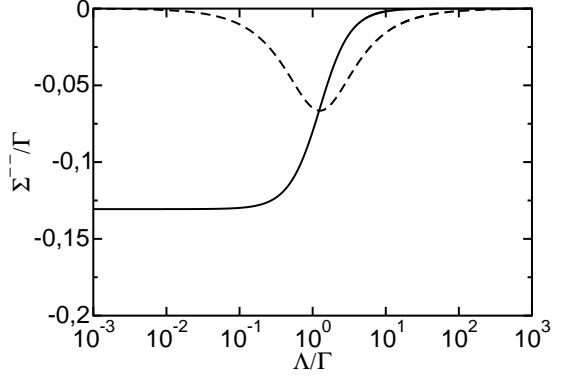


FIG. 4: Flow of $\Sigma^{--, \Lambda}/\Gamma$ with $\Lambda/\Gamma = 1$, $V_G/\Gamma = 0.5$, and $V_B = 0$. The full curve shows the real part, the dashed the imaginary part of Σ^{--} .

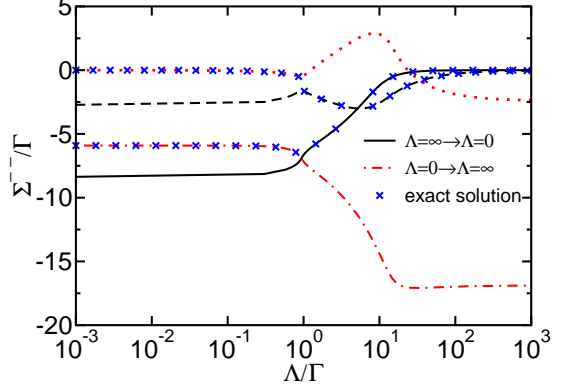


FIG. 5: (color online) Flow of $\Sigma^{--, \Lambda}/\Gamma$ with $U/\Gamma = 15$, $V_G/\Gamma = 6$, and $V_B = 0$. The full and dashed curves show real and imaginary part obtained from the integration $\Lambda = \infty \rightarrow \Lambda = 0$, the dashed-dotted and dotted curves real and imaginary part obtained from an integration $\Lambda = 0 \rightarrow \Lambda = \infty$, using the solution from (45) as initial value for Σ^{--} . The crosses denote the analytical solution (44).

result in such a situation is shown in Fig. 5. The different curves were obtained as follows: The full and dashed ones from the numerical solution starting with $\Sigma^{--} = 0$ at $\Lambda \rightarrow \infty$, the dash-dotted and dotted by integrating the differential equation (43) backwards from $\Lambda = 0$ with the correct solution for $\Lambda = 0$ as given by formula (45) as initial value. The crosses finally are the results from the analytical solution (44). Evidently, there exists a crossing of different branches of solutions to the differential

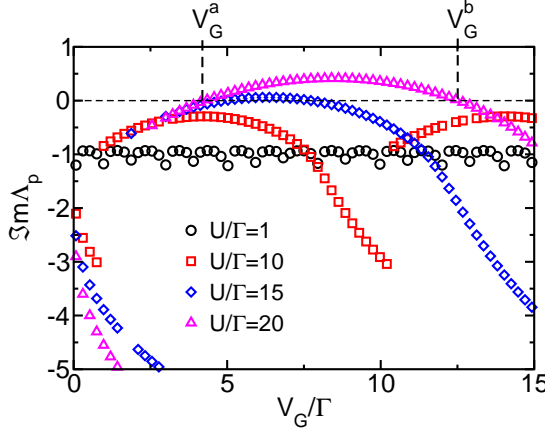


FIG. 6: (color online) Imaginary part of Λ_p determined from (44) and $V_G + \Sigma^{--,\Lambda_p} = \Lambda_p + i\Gamma$ for different values of U and $V_B = 0$ as function of V_G . For $U/\Gamma = 15$ and 20 there exist an interval $[V_G^a, V_G^b]$ where $\Im m\Lambda_p > 0$, while for small U or $V_G \notin [V_G^a, V_G^b]$ we always have $\Im m\Lambda_p < 0$.

equation for $\Lambda/\Gamma \approx 1$ and the numerical solution with starting point $\Lambda = \infty$ picks the wrong one as $\Lambda \rightarrow 0$. The reason for this behavior is that for large U there exists a certain V_G^a such that $V_G^a + \Sigma^{--,\Lambda_p} = \Lambda_p + i\Gamma$ with real Λ_p , resulting in a pole in the differential equation (43). For $V_G \neq V_G^a$ this pole does not appear for real Λ_p , but as shown in Fig. 6 $\Im m\Lambda_p$ changes sign at V_G^a , which in turn induces a sign change on the right hand side of the differential equation, leading to the behavior observed in Fig. 5. Note that there also exists a second critical value V_G^b such that for $V_G > V_G^b$ we find $\Im m\Lambda_p < 0$ and the instability has vanished again.

Obviously, this instability limits the applicability of the present approximation to small values of U . This is different from the imaginary-time approach by Andergassen *et al.*,³⁷ where this simple approximation leads to qualitative correct results even for values of U significantly larger than Γ .

b. Non-equilibrium. We now turn to the case of finite bias voltage V_B . As a typical example, the flow of Σ^{--} for $U/\Gamma = 1$ (full and dashed curves) and 5 (dashed-dotted and dotted curves) for $V_G/\Gamma = 0.5$ at $V_B/\Gamma = 0$ (equilibrium) and $V_B/\Gamma = 1$ is shown in Fig. 7. Since the results for Σ^{++} are related to those for Σ^{--} by $\Sigma^{++} = -[\Sigma^{--}]^*$ we do not show them here. The V_B dependence of the curves for $\Re e[\Sigma^{--}]$ (thick lines) looks sensible. For $V_B \neq 0$ an imaginary part of order U^2 is generated in the flow which does not vanish for $\Lambda \rightarrow 0$ (see the thin dotted line). Causality requires that the relation

$$\Sigma^{--}(\omega) + \Sigma^{++}(\omega) = -[\Sigma^{--}(\omega) + \Sigma^{++}(\omega)] \quad (46)$$

must hold. Because of $\Sigma^{--}(\omega) = \Sigma^{++}(\omega) = 0$, the finite imaginary part of $\Sigma^{\alpha\alpha}$ leads to a breaking of the condition (46) to order U^2 at the end of the FRG flow. This

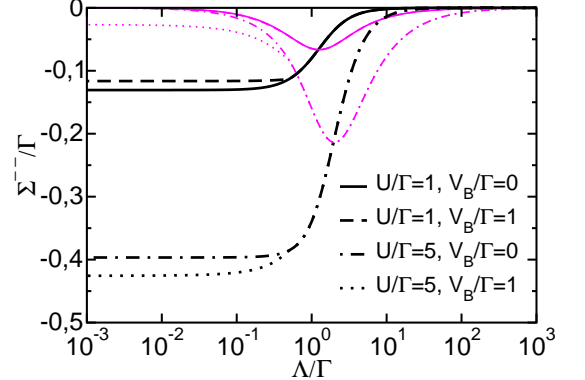


FIG. 7: (color online) Flow of $\Sigma^{--,\Lambda}/\Gamma$ with Λ for $U/\Gamma = 1$ and 5 for $V_G/\Gamma = 0.5$ at $V_B/\Gamma = 0$ and 1 (thick curves: real part; thin curves: imaginary part). The curve for $\Im \Sigma^{--,\Lambda}/\Gamma$ at $U/\Gamma = 1$ and $V_B/\Gamma = 1$ (thin dashed line) lies on top of the corresponding zero bias curve and is thus not visible.

is consistent with the fact that by neglecting the flow of the vertex terms of order U^2 are only partially kept in the present FRG truncation scheme. To avoid any confusion we emphasize that our RG method is different from any low-order perturbation theory. The weak breaking of causality can also be understood as a consequence of our approximation leading to a *complex*, energy-independent self-energy: The off-diagonal components, being related to the distribution functions for electrons and holes, respectively, in general have different support on the energy axis. The energy independence makes it impossible to respect this requirement here.

For our further discussion the order U^2 violation of (46) means that we may not rely on relations like (8)-(10) but have to work with $G^{\alpha\beta}$, thus the somewhat unusual formula (35). A naive application of $\Sigma^R = \Sigma^{--} - \Sigma^{+-}$ and use of $G_d^{+-} - G_d^{--} = 2i\Im m G_d^R$ would have led to unphysical results. That the difference $G_d^{+-} - G_d^{--}$ is still sensible can be seen from a straightforward evaluation leading to

$$G_d^{+-}(\omega) - G_d^{--}(\omega) = \frac{\Gamma}{-2i|\omega - V_G + i\Gamma[1 - F(\omega)] - \Sigma^{--}|^2 + \Gamma^2 F(\omega)F(-\omega)} \quad (47)$$

$$F(\omega) := f_L(\omega) + f_R(\omega)$$

which is purely imaginary with a definite sign. Inserting the expression (47) into the formula (35), one can calculate the current and thus the conductance. Since we are working at $T = 0$, an explicit expression for the current of the cutoff free problem (at $\Lambda = 0$) can be obtained by noting that with $\mu_L = V_B/2$, $\mu_R = -V_B/2$ one has $f_L(\omega) - f_R(\omega) = \Theta(V_B/2 - |\omega|)$ and $F(\pm\omega) = 1$ for

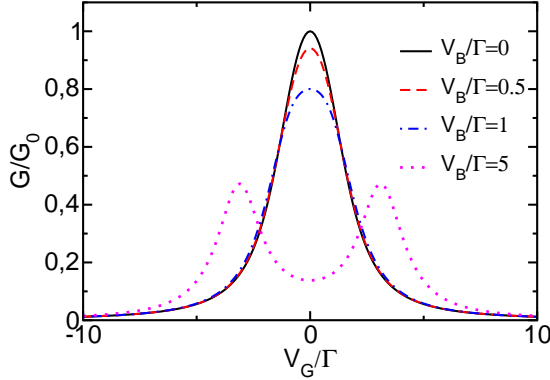


FIG. 8: (color online) Conductance normalized to $G_0 = 2e^2/h$ as function of V_G for $U/\Gamma = 2$ and several values of the bias voltage V_B .

$\omega \in [-V_B/2, V_B/2]$, which leads to

$$\begin{aligned} J &= \frac{e\Gamma^2}{\pi\hbar} \int_{-V_B/2}^{V_B/2} d\omega \frac{1}{|\omega - V_G - \Sigma^{--}|^2 + \Gamma^2} \\ &= \frac{e\Gamma}{\pi\hbar} \frac{\Gamma}{\Gamma^*} \sum_{s=\pm 1} s \arctan \left(\frac{V_G^* + s\frac{V_B}{2}}{\Gamma^*} \right) \end{aligned} \quad (48)$$

with the abbreviations

$$V_G^* := V_G + \Re \Sigma^{--} \quad (49)$$

$$\Gamma^* := \sqrt{\Gamma^2 + (\Im m \Sigma^{--})^2}, \quad (50)$$

i.e. the expression for the non-interacting system with renormalized parameters V_G^* and Γ^* . Note that this result is actually quite reasonable thus supporting our claim that the use of $\Sigma^{\alpha\beta}$ (or $G_d^{\alpha\beta}$) in the calculation of physical properties is permissible.

An example for the differential conductance obtained from (48) for $U/\Gamma = 2$ as function of V_G for several values of V_B is shown in Fig. 8, where $G_0 = 2e^2/h$. Increasing V_B leads, as expected, first to a decrease of the conductance close to $V_G = 0$ and later to a splitting of order V_B . Since we will discuss a more refined scheme including the flow of the vertex next, we do not intend to dwell too much on the results of this simplest approximation. We note in passing that for $V_G = 0$ due to particle-hole symmetry we obtain from the differential equation (42) that $\Sigma^{--} = 0$ independent of U . Consequently the current J calculated via (48) and the conductance are independent of U , too, and given by the corresponding expressions for the non-interacting system. As we will see in the next section, this deficiency will be cured by the approximate inclusion of the vertex flow.

In the present approximation the current conservation $\Delta J = 0$ holds for all parameters as $\Sigma^{-+} = \Sigma^{+-} = 0$ (cf. Eq. (36)).

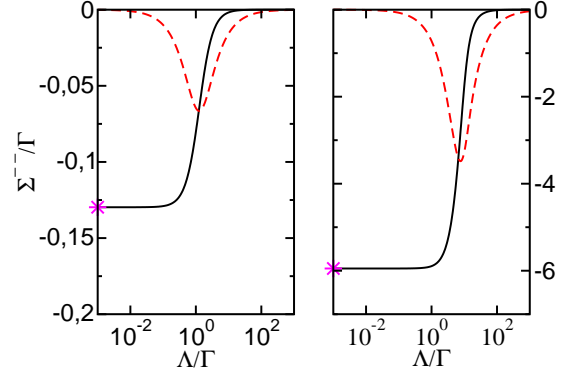


FIG. 9: (color online) Flow of $\Sigma^{--,\Lambda}/\Gamma$ for Λ for $U/\Gamma = 1$ (left panel) and $U/\Gamma = 15$ (right panel) at $V_G = U/2$ and $V_B = 0$. The full curves show the real part, the dashed the imaginary part of Σ^{--} . The stars at the vertical axis denote the values as obtained from the imaginary-time FRG.

C. Flowing vertex

A more refined approximation is obtained when we insert the flowing two-particle vertex γ_2 as given by expression (B2) in the calculation of the self-energy with (23). By this we introduce an energy-dependence.²³ However, because the size of the resulting system of differential equations becomes extremely large, we in addition adopt the approximation of an energy-independent vertex function γ_2 .³⁸ The resulting expression for the self-energy (see Appendix B) is

$$\frac{d}{d\Lambda} \Sigma^{\alpha\beta,\Lambda} = -\frac{1}{2\pi} \sum_{s=\pm 1} G_d^{\gamma\delta}(s\Lambda) (2U^{\alpha\delta\beta\gamma} - U^{\delta\alpha\beta\gamma}), \quad (51)$$

where the combination of $U^{\alpha\delta\beta\gamma}$ is determined by the spin sum in (23) and the flow of $U^{\alpha\delta\beta\gamma}$ is given by the expression (B3). As has been observed by Karrasch *et al.*,³⁸ this approximation leads to a surprisingly accurate description of the transport properties in equilibrium. In particular it is far superior to the lowest order approximation including only the unrenormalized vertex.

c. Equilibrium. We again begin with the discussion of the solution to (51) in equilibrium. The results are shown in Fig. 9 for $U/\Gamma = 1$ (left panel) and $U/\Gamma = 15$ (right panel) for $V_G = U/2$. Since $\Sigma^{++} = -[\Sigma^{--}]^*$ only one component is shown. The stars denote the solutions of the imaginary-time equations according to Ref. 38. Note that for $U/\Gamma = 15$ and $V_G/\Gamma > 6$ the simple approximation (42) showed an instability, while with the flowing vertex the system is stable even for these large values of U and reproduces the correct equilibrium solutions for $\Lambda \rightarrow 0$.³⁸ The reason is that the flow of the vertex reduces the resulting effective interaction below the critical value in the instability region.³⁸

d. Non-equilibrium. For the same parameters as in Fig. 9 we present the resulting flow with finite bias $V_B/\Gamma = 1$ in Fig. 10. In addition to the curves for real

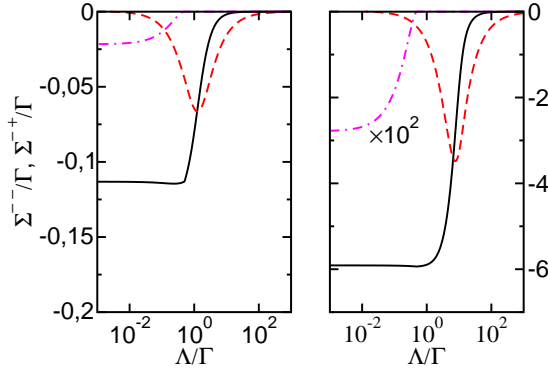


FIG. 10: (color online) Flow of $\Sigma^{--,\Lambda}/\Gamma$ and $\Sigma^{-+,\Lambda}$ for $U/\Gamma = 1$ (left panel) and $U/\Gamma = 15$ (right panel), $V_G/\Gamma = U/2$ and $V_B/\Gamma = 1$. The full curves show the real part, the dashed the imaginary part of Σ^{--} , the dot-dashed the imaginary part of Σ^{-+} . Note that the real part for the latter is zero.

(solid lines) and imaginary part (dashed lines) of Σ^{--} a third curve is displayed, the imaginary part of Σ^{-+} (dashed-dotted lines), which now is generated during the flow. Note that $\Re \Sigma^{-+} = 0$ and $\Sigma^{+-} = [\Sigma^{-+}]^*$. Furthermore, we always find $\Im m \Sigma^{-+} < 0$. For $U/\Gamma = 15$ (right panel in Fig. 10) we have rescaled $\Im m \Sigma^{-+}$ by a factor 10^2 to make it visible on the scale of Σ^{--} . Since $\Sigma^{\alpha\beta}$ is a complex energy independent quantity (46) is again not fulfilled. We note that the error is still of order

U^2 , but for a fixed set of parameters significantly smaller than in the simplest truncation scheme discussed above.

The energy-independence of the self-energy allows to derive an analytical expression for the current at $T = 0$ similar to Eq. (48), which due to the appearance of Σ^{-+} now becomes

$$J = \frac{e\Gamma}{\pi\hbar} \frac{\tilde{\Gamma}}{\Gamma^*} \sum_{s=\pm 1} s \arctan \left(\frac{V_G^* + s\frac{V_B}{2}}{\Gamma^*} \right) \quad (52)$$

with V_G^* as in (49) and

$$\tilde{\Gamma} = \Gamma - \Im m \Sigma^{-+} > \Gamma$$

$$\Gamma^* = \sqrt{\tilde{\Gamma}^2 + (\Im m \Sigma^{--})^2} ;$$

where $\Sigma^{\alpha\beta}$ is taken at $\Lambda = 0$. Thus, the only change to the expression (48) is a formal replacement $\Gamma \rightarrow \tilde{\Gamma}$ in $\hbar J/\Gamma$. Again, the formula is of the same structure as for the non-interacting case with V_G and Γ replaced by renormalized parameters. However, the two self-energy contributions Σ^{--} and Σ^{-+} enter distinctively different in the expression for the current. While $\Im m \Sigma^{--}$ solely plays the role of an additional life-time broadening, $\Im m \Sigma^{-+}$ directly modifies the tunneling rate both in the prefactor of J and in the expression for the life-time broadening.

A problem occurs when using the results of the present approximation in Eq. (36), leading to

$$\Delta J = 2 \frac{e\Gamma}{\pi\hbar} \int_{-\infty}^{\infty} d\omega \frac{\Im m \Sigma^{-+} [1 - F(\omega)]}{|\omega - V_G + i\Gamma [1 - F(\omega)] - \Sigma^{--}|^2 + [\Gamma F(-\omega) + \Im m \Sigma^{+-}] [\Gamma F(\omega) - \Im m \Sigma^{-+}]} . \quad (53)$$

The requirement $\Delta J = 0$ is only fulfilled for $V_G = 0$, because then $\Sigma^{--} = 0$ and the integrand is asymmetric with respect to ω . Thus our approximation of an energy-independent flowing vertex violates current conservation for $V_G \neq 0$ in non-equilibrium. We verified that $\Delta J \sim U^2$ which is consistent with the fact that not all terms of order U^2 are kept in our truncated FRG procedure. How does ΔJ behave in the limit $V_B \rightarrow 0$? To see this we note that, because $\Im m \Sigma^{-+}$ does not depend on the sign of V_B and furthermore goes to zero as $V_B \rightarrow 0$, $\Im m \Sigma^{-+} \xrightarrow{V_B \rightarrow 0} V_B^2$. Consequently, $\Delta J \xrightarrow{V_B \rightarrow 0} V_B^2$ and hence the violation of current conservation vanishes in the linear response regime $V_B \rightarrow 0$.

In Fig. 11 we show the current at $V_G = 0$ as function of V_B for $U/\Gamma = 1, 6$ and 15 . With increasing U the current for intermediate V_B is strongly suppressed. In addition there occurs a structure at low V_B , which turns into a region of negative differential conductance with increasing U . The appearance of such a shoulder in

the current was observed in other calculations^{48,49,52} as well. However, whether the negative differential conductance we find for still larger values of U (c.f. Fig. 12) is a true feature of the model or rather an artifact of the approximations used is presently not clear and should be clarified in further investigations. Note, however, that negative differential conductance has also been observed in a slave-boson treatment of the model.⁵⁹

Keeping $V_G = 0$ fixed, we can calculate the conductance $G = dJ/dV_B$ as function of V_B for different values of U . The results are collected in Fig. 12. In contrast to the simple approximation without flow of the vertex, the conductance is now strongly dependent on U , except for $V_B = 0$, where due to the unitarity limit at $T = 0$ we always find $G = G_0 = 2e^2/h$. As already anticipated from the current in Fig. 11, a minimum in G starts to form around $V_B/\Gamma \approx 0.5$ for $U/\Gamma > 5$, which is accompanied by a peak at $V_B/\Gamma \approx 2$. Note that a similar behavior in the conductance was observed in a perturba-

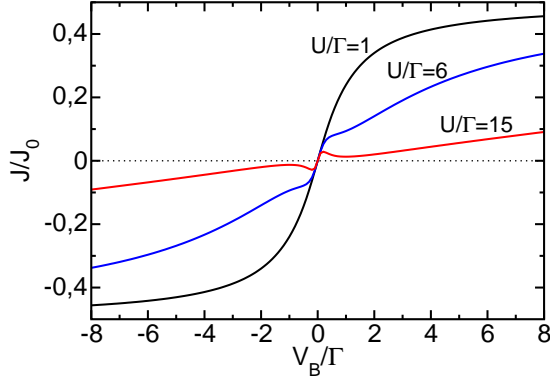


FIG. 11: (color online) Current normalized to $J_0 := G_0 \frac{\Gamma}{e}$ as function of V_B for $U/\Gamma = 1, 6$ and 15 and $V_G = 0$. For $U/\Gamma = 15$ we find a region of negative differential conductance in the region $|V_B/\Gamma| \approx 0.5$ (c.f. Fig. 12).

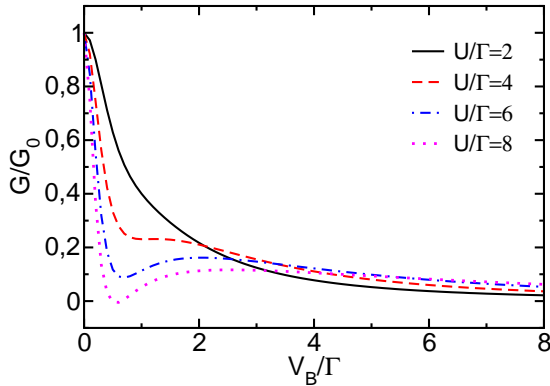


FIG. 12: (color online) Differential conductance G as function of V_B for $V_G = 0$ and various values of U . For $U/\Gamma > 5$ a distinct minimum around $V_B/\Gamma \approx 0.5$ appears.

tional treatment,⁵² which in contrast to our current approximation involves the full energy-dependence in the self-energy. This at least qualitative agreement – we of course cannot resolve structures like the Hubbard bands with an energy independent self-energy – again supports our claim that despite the violation of the relation (46) we can obtain reasonable results from $G^{\alpha\beta}$.

We finally discuss the variation of the conductance with V_G for fixed U and V_B . We again emphasize, that for $V_G \neq 0$, $\Delta J = 0$ only holds to leading order in U . In Fig. 13 we present the curves for two different values of U , namely $U/\Gamma = 1$ (upper panel in Fig. 13) and $U/\Gamma = 15$ (lower panel in Fig. 13).⁵⁶ In the former case, the variation of G with V_B is rather smooth, as is to be expected from the current in Fig. 11. For large U , we observe an extended plateau at zero bias, which is a manifestation of the fact that in the strong coupling regime a pinning of spectral weight at the Fermi energy occurs. This feature is also observed in the imaginary-time FRG as well as in NRG calculations.³⁸ Increasing V_B quickly

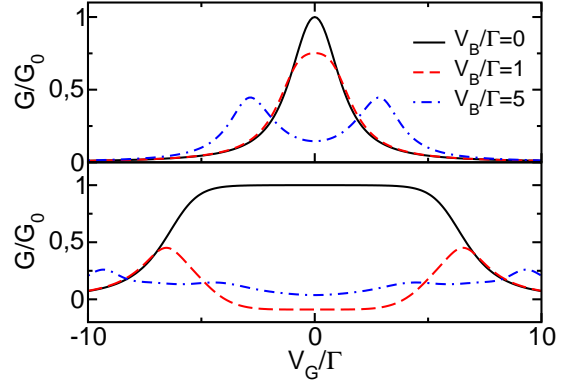


FIG. 13: (color online) Differential conductance G as function of V_G for different values of V_B and $U/\Gamma = 1$ (upper panel) and $U/\Gamma = 15$ (lower panel). Note the extended plateau at $V_B = 0$ for $U/\Gamma = 15$, which is a manifestation of the pinning of spectral weight at the Fermi level.

leads to a similarly extended region of negative differential conductance, which, assuming that this result is a true feature of the model, therefore seems to be linked to the “Kondo” pinning. We note that it is unlikely that the appearance of the negative differential conductance is related to the breaking of current conservation at order U^2 as it also appears for $V_G = 0$ where $\Delta J = 0$. For large V_B multiple structures appear in G , which are related to the energy scales V_B and U .

IV. SUMMARY AND CONCLUSION

Starting from a generating functional proposed by Kameneev⁴² we have derived an infinite hierarchy of differential equations for the vertex functions of an interacting quantum mechanical many-body system in non-equilibrium (see also Ref. 24,25). The major difference to the imaginary-time formulation comes from the use of Keldysh Green functions, introducing an additional matrix structure to the problem. Our formulation is sufficiently general that it allows to treat bosonic and fermionic models with or without explicit time dependence and at $T \geq 0$. Since the FRG leads to an infinite hierarchy of coupled differential equations, one has to introduce approximations, at least a truncation at a certain level, typically for $m = 2$. As has been demonstrated in Ref. 23 for the imaginary-time FRG one can solve the remaining system for simple models like the SIAM numerically, thus keeping the full energy-dependence. Note that due to the fact that the vertex function carries three *continuous* frequency arguments in addition to the discrete quantum numbers of the system, such a calculation can become computationally quite expensive. To reduce the numerical effort, further approximations can be introduced. A particularly important and successful one is obtained by neglecting the energy dependence of the ver-

tex functions,^{37,38} which already leads to a surprisingly accurate description of local and transport properties of interacting quantum dots in the linear response regime.

We applied our technique to the SIAM with finite bias voltage in the stationary state. It turned out, that for the simplest approximation, i.e. a truncation at the level $m = 1$, the analytic structure of the differential equation led to problems in the numerical solution. In addition, this approximation led to a violation of the causality relation (46) to order U^2 . The first problem was resolved by including the two-particle vertex in the flow at least up to the largest interaction considered here ($U/\Gamma = 15$). At the present stage this was for computational reasons done by assuming it to be energy-independent, yielding again an energy-independent self-energy. Although this approximation also violates (46) to order U^2 for a fixed

parameter set the error is significantly smaller compared to the $m = 1$ scheme. We were able to obtain reasonable expressions and numerical results for the current and the conductance using the functions $G^{\alpha\beta}(\omega)$ instead of $G^R(\omega)$ in the current formula. We reproduced non-equilibrium features of the current and differential conductance known from the application of other approximate methods to the SIAM. In the more advanced truncation scheme and for $V_G \neq 0$, $\Delta J = 0$ only holds to leading order in U . This defect can be traced back to the energy independence of the two-particle vertex, leading to finite, but energy-independent Σ^{-+} and Σ^{+-} . By a close inspection of formula (36), however, it is easy to see that this deficiency can for example be cured by assuming a coarse-grained energy dependence of the form

$$\omega < -\frac{V_B}{2} : F(\omega) = 2 \Rightarrow \Im m \Sigma^{+-} = 0, \Sigma^{-+} = \text{const.} \quad (54)$$

$$-\frac{V_B}{2} < \omega < \frac{V_B}{2} : F(\omega) = 1 \Rightarrow \Im m \Sigma^{+-} = -\Im m \Sigma^{-+} = \text{const.} \quad (55)$$

$$\frac{V_B}{2} < \omega : F(\omega) = 0 \Rightarrow \Im m \Sigma^{-+} = 0, \Sigma^{+-} = \text{const.} \quad (56)$$

and corresponding energy dependencies for Σ^{--} and Σ^{++} . Note that such an approximation will quite likely also reestablish causality (46). Work along this line is in progress.

Including finite temperature, magnetic field etc. in the calculations of transport is easily possible, as well as the extension to more complicated “impurity” structures (see e.g. Ref. 38). Note that the latter aspect typically is a rather cumbersome step for other methods like perturbation theories or in particular numerical techniques.

Our present stage of work should mainly be seen as a “proof of principle”. Already for the SIAM there remain a variety of fundamental things to do; like the implementation of the energy-dependence in the calculations, which then should cure the violation of charge conservation and causality (46); or implementing a reasonable cutoff scheme for time-dependent problems off equilibrium, e.g. to calculate current transients. Despite its current limitations we expect the real-time non-equilibrium formulation of the FRG to be a useful tool to understand non-equilibrium features of mesoscopic systems, just like the imaginary-time version in the calculation of equilibrium properties.

Acknowledgments

We acknowledge useful conversations with H. Schoeller, S. Jakobs, S. Kehrein, J. Kroha, H. Monien,

A. Schiller, A. Dirks, J. Freericks, K. Ueda, T. Fujii, K. Thygesen, and F.B. Anders. This work was supported by the DFG through the collaborative research center SFB 602. Computer support was provided through the Gesellschaft für wissenschaftliche Datenverarbeitung in Göttingen and the Norddeutsche Verbund für Hoch- und Höchstleistungsrechnen.

APPENDIX A: DERIVATION OF THE FLOW EQUATIONS

Although the following derivation is mainly equivalent to the one presented in Ref. 23, the appearance of the factor i in the real-time formulation of the generating functional leads to some changes in signs and prefactors i in the equations. We thus think it helpful to the reader to repeat the derivation.

As a first step we differentiate $\mathcal{W}^{c,\Lambda}$ with respect to Λ , which after straightforward algebra leads to

$$\frac{d}{d\Lambda} \mathcal{W}^{c,\Lambda} = \zeta \operatorname{Tr} (\mathcal{Q}^\Lambda \mathcal{G}^{0,\Lambda}) + (i\zeta) \operatorname{Tr} \left(\mathcal{Q}^\Lambda \frac{\delta^2 \mathcal{W}^{c,\Lambda}}{\delta \bar{\eta} \delta \eta} \right) + i \left(\frac{\delta \mathcal{W}^{c,\Lambda}}{\delta \eta}, \mathcal{Q}^\Lambda \frac{\delta \mathcal{W}^{c,\Lambda}}{\delta \bar{\eta}} \right), \quad (\text{A1})$$

with

$$\mathcal{Q}^\Lambda = \frac{d}{d\Lambda} [\mathcal{G}^{0,\Lambda}]^{-1}. \quad (\text{A2})$$

Considering ϕ and $\bar{\phi}$ as the fundamental variables we obtain from Eq. (16)

$$\frac{d}{d\Lambda} \Gamma^\Lambda (\{\bar{\phi}\}, \{\phi\}) = -\frac{d}{d\Lambda} \mathcal{W}^{c,\Lambda} (\{\bar{\eta}^\Lambda\}, \{\eta^\Lambda\}) - i \left(\bar{\phi}, \frac{d}{d\Lambda} \eta^\Lambda \right) - i \left(\frac{d}{d\Lambda} \bar{\eta}^\Lambda, \phi \right) + i (\bar{\phi}, \mathcal{Q}^\Lambda \phi). \quad \boxed{\quad}$$

Applying the chain rule and using Eq. (A1) this leads to

$$\frac{d}{d\Lambda} \Gamma^\Lambda = -\zeta \operatorname{Tr} (\mathcal{Q}^\Lambda \mathcal{G}^{0,\Lambda}) - (i\zeta) \operatorname{Tr} \left(\mathcal{Q}^\Lambda \frac{\delta^2 \mathcal{W}^{c,\Lambda}}{\delta \bar{\eta}^\Lambda \delta \eta^\Lambda} \right),$$

where the last term in Eq. (16) cancels a corresponding

contribution arising in (A1) thus a posterior justifying the inclusion of this term.

Using the well known relation⁴³ between the second functional derivatives of Γ and \mathcal{W}^c we obtain the functional differential equation

$$\frac{d}{d\Lambda} \Gamma^\Lambda = -\zeta \operatorname{Tr} (\mathcal{Q}^\Lambda \mathcal{G}^{0,\Lambda}) - \operatorname{Tr} \left(\mathcal{Q}^\Lambda \mathcal{V}_{\bar{\phi},\phi}^{1,1} (\Gamma^\Lambda, \mathcal{G}^{0,\Lambda}) \right), \quad (\text{A3})$$

where $\mathcal{V}_{\bar{\phi},\phi}^{1,1}$ stands for the upper left block of the matrix

$$\mathcal{V}_{\bar{\phi},\phi} (\Gamma^\Lambda, \mathcal{G}^\Lambda) = \begin{pmatrix} i \frac{\delta^2 \Gamma^\Lambda}{\delta \bar{\phi} \delta \phi} - \zeta [\mathcal{G}^{0,\Lambda}]^{-1} & i \frac{\delta^2 \Gamma^\Lambda}{\delta \bar{\phi} \delta \bar{\phi}} \\ (i\zeta) \frac{\delta^2 \Gamma^\Lambda}{\delta \phi \delta \phi} & - \left[i \frac{\delta^2 \Gamma^\Lambda}{\delta \phi \delta \phi} + \left[[\mathcal{G}^{0,\Lambda}]^{-1} \right]^t \right] \end{pmatrix}^{-1} \quad (\text{A4})$$

and the upper index t denotes the transposed matrix. To obtain differential equations for the γ_m^Λ which include self-energy corrections we express $\mathcal{V}_{\bar{\phi},\phi}$ in terms of \mathcal{G}^Λ instead of $\mathcal{G}^{\Lambda,0}$. This is achieved by defining

$$\mathcal{U}_{\bar{\phi},\phi} = i \frac{\delta^2 \Gamma^\Lambda}{\delta \bar{\phi} \delta \phi} - \gamma_1^\Lambda$$

and using

$$\mathcal{G}^\Lambda = \left[[\mathcal{G}^{0,\Lambda}]^{-1} - \zeta \gamma_1^\Lambda \right]^{-1}, \quad (\text{A5})$$

which leads to

$$\frac{d}{d\Lambda} \Gamma^\Lambda = -\zeta \operatorname{Tr} (\mathcal{Q}^\Lambda \mathcal{G}^{0,\Lambda}) + \zeta \operatorname{Tr} \left(\mathcal{G}^\Lambda \mathcal{Q}^\Lambda \tilde{\mathcal{V}}_{\bar{\phi},\phi}^{1,1} (\Gamma^\Lambda, \mathcal{G}^\Lambda) \right), \quad (\text{A6})$$

with

$$\tilde{\mathcal{V}}_{\bar{\phi},\phi} (\Gamma^\Lambda, \mathcal{G}^\Lambda) = \left[\mathbf{1} - \begin{pmatrix} \zeta \mathcal{G}^\Lambda & 0 \\ 0 & [\mathcal{G}^\Lambda]^t \end{pmatrix} \begin{pmatrix} \mathcal{U}_{\bar{\phi},\phi} & i \frac{\delta^2 \Gamma^\Lambda}{\delta \bar{\phi} \delta \phi} \\ (i\zeta) \frac{\delta^2 \Gamma^\Lambda}{\delta \phi \delta \phi} & \zeta \mathcal{U}_{\bar{\phi},\phi}^t \end{pmatrix} \right]^{-1}. \quad (\text{A7})$$

For later applications it is important to note that $\mathcal{U}_{\bar{\phi},\phi}$ as well as $\frac{\delta^2 \Gamma^\Lambda}{\delta \bar{\phi} \delta \phi}$ and $\frac{\delta^2 \Gamma^\Lambda}{\delta \phi \delta \phi}$ are at least quadratic in the

external sources. The initial condition for the exact functional differential equation (A6) can either be obtained by lengthy but straightforward algebra, which we are not going to present here or by the following simple argument: at $\Lambda = \Lambda_0$, $\mathcal{G}^{0,\Lambda_0} = 0$ (no degrees of freedom are “turned on”) and in a perturbative expansion of the $\gamma_m^{\Lambda_0}$

the only term which does not vanish is the bare 2-particle vertex. We thus find

$$\Gamma^{\Lambda_0}(\{\bar{\phi}\}, \{\phi\}) = S_{\text{int}}(\{\bar{\phi}\}, \{\phi\}) . \quad (\text{A8})$$

By expanding $\tilde{\mathcal{V}}$ Eq. (A7) in a geometric series

$$\tilde{\mathcal{V}} = 1 + \zeta G^\Lambda \mathcal{U}_{\bar{\phi}, \phi} + G^\Lambda \mathcal{U}_{\bar{\phi}, \phi} G^\Lambda \mathcal{U}_{\bar{\phi}, \phi} + \zeta^3 i^2 G^\lambda \frac{\delta^2 \Gamma}{\delta \bar{\phi} \delta \phi} [G^\Lambda]^t \frac{\delta^2 \Gamma}{\delta \phi \delta \phi} + \dots \quad (\text{A9})$$

and Γ^Λ in a Taylor series with respect to the external sources

$$\Gamma^\Lambda(\{\bar{\phi}\}, \{\phi\}) = \sum_{m=0}^{\infty} \frac{(i\zeta)^m}{(m!)^2} \sum_{\xi'_1, \dots, \xi'_m} \sum_{\xi_1, \dots, \xi_m} \gamma_m^\Lambda(\xi'_1, \dots, \xi'_m; \xi_1, \dots, \xi_m) \bar{\phi}_{\xi'_1} \dots \bar{\phi}_{\xi'_m} \phi_{\xi_m} \dots \phi_{\xi_1} . \quad (\text{A10})$$

an exact infinite hierarchy of flow equations for the γ_m^Λ can be obtained. For example, the flow equation for the single-particle vertex γ_1 (the self-energy) can be obtained by taking the expansion (A9) up to first order in \mathcal{U} , insert it into (A6), replace Γ^Λ on both sides with the expansion (A10) and compare expressions with the same powers in the fields, i.e. for γ_1 up to order $m = 1$. This procedure leads to the expression (20).

APPENDIX B: FLOW EQUATION FOR THE VERTEX FUNCTION

To obtain the flow equation for $\dot{\Sigma}$ we have expanded Eq. (A7) in a geometric series ($n = 1$) up to first order

$$\frac{\partial}{\partial \Lambda} \gamma^{\alpha\beta\gamma\delta}(1', 2'; 1, 2) = \sum_{3, 3'} \sum_{4, 4'} \sum_{\mu, \nu, \rho, \eta} \left(G^{\rho\eta}(3', 3) S^{\nu\mu}(4, 4') [\gamma^{\alpha\beta\rho\nu}(1', 2'; 3, 4) \gamma^{\eta\mu\gamma\delta}(3', 4'; 1, 2)] - G^{\eta\rho}(3, 3') S^{\nu\mu}(4, 4') [\gamma^{\alpha\mu\gamma\eta}(1', 4'; 1, 3) \gamma^{\rho\beta\nu\delta}(3', 2'; 4, 2) + \gamma^{\alpha\rho\gamma\nu}(1', 3'; 1, 4) \gamma^{\mu\beta\eta\delta}(4', 2'; 3, 2) - \gamma^{\beta\mu\gamma\eta}(2', 4'; 1, 3) \gamma^{\rho\alpha\nu\delta}(3', 1'; 4, 2) - \gamma^{\beta\rho\gamma\nu}(2', 3'; 1, 4) \gamma^{\mu\alpha\eta\delta}(4', 1'; 3, 2)] \right) , \quad (\text{B1})$$

where the contribution involving γ_3 was replaced by its initial value, i.e. $\gamma_3 = 0$. The sums over the dynamical indices must be read as sums or integrals over all possible variables such as time or frequency, spin, etc. The main difference to equilibrium is the presence of mixed contractions for the Keldysh indices of the matrices \hat{G} and \hat{S} and the four-index tensors γ_2 , which in practice

and Γ^Λ (A10) in the external sources up to the order $m = 2$. In order to find the flow equation for the vertex function, $\dot{\gamma}_2$, we just have to proceed one step further, viz expand (A7) up to the second order and Γ^Λ up to third. After comparison of the terms with the same power in the fields we obtain expression similar to equilibrium (see Eq. (15) by Karrasch *et al.*³⁸ and Fig. 3):

add two indices more to the original equation obtained by Karrasch *et al.*³⁸.

Before manipulating the expression (B1) further, some remarks on the relations among the dynamical and the Keldysh indices and the tensor structure of γ_2 with respect to the permutation of two Keldysh indices is in place. From the derivation of the flow-equations, each

Keldysh index is connected to a dynamical one, for example in $G^{\nu\mu}(4,4')$ the Keldysh index ν is linked to 4 and μ to $4'$. This means that if we permute $\widehat{\nu\mu} \rightarrow \widehat{\mu\nu}$ and then $\widehat{4,4'} \rightarrow \widehat{4',4}$, too. It's also important to remember that the permutation of each dynamical index induces a minus sign in the vertex (antisymmetry for Fermions), which is not true for the permutation of two Keldysh indices, because they do not represent any physical variable such as impulse, spin etc.

We now come back to the expression (B1). In order to simplify it further, we may follow the same steps as in Ref. 23,38 and thus just give a brief description of the procedure: In the stationary state we wish to consider, spin and energy conservation requires the dynamical indices of G and \mathcal{S} to be equal, $3 = 3'$ and $4 = 4'$. Note that this is *not* true for the Keldysh indices! In this way we get rid of the two integrals $d\omega_{4'}$ and $d\omega_{3'}$. Introducing again a sharp frequency cutoff as in Eq. (40) and using Morris

lemma,²⁰ we can rewrite the matrix product component by component as

$$\begin{aligned} G^\Lambda(\omega)\mathcal{S}^\Lambda(\omega') &\rightarrow \frac{\theta(|\omega| - \Lambda)}{\mathcal{G}^0(\omega) - \Sigma^\Lambda(\omega)} \frac{\delta(|\omega'| - \Lambda)}{\mathcal{G}^0(\omega') - \Sigma^\Lambda(\omega')} \\ &\equiv \frac{1}{2}\delta(|\omega'| - \Lambda)G(\omega)G(\omega') . \end{aligned}$$

Now the delta function combined with energy conservation can be used to perform the remaining integrals over $d\omega_4$ and $d\omega_3$.

Up to now the manipulations have been completely general and still involve the full frequency dependence of the vertex and self-energy. In order to keep things simple, the evaluation of the full set of equations is very cumbersome even in equilibrium,²³ we now restrict the evaluation to the Fermi energy, i.e. set the external frequencies in the arguments of γ_2 to zero. This leads to the final expression

$$\begin{aligned} \frac{\partial}{\partial\Lambda}\gamma_{1',2';1,2}^{\alpha\beta\gamma\delta} &= \frac{1}{4\pi} \sum_{\omega=\pm\Lambda} \sum_{3,4} \sum_{\mu,\nu\rho,\eta} \left(G_3^{\rho\eta}(-\omega)G_4^{\nu\mu}(\omega)\gamma_{1',2';3,4}^{\alpha\beta\rho\nu}\gamma_{3',4';1,2}^{\eta\mu\gamma\delta} - \right. \\ &\quad G_3^{\eta\rho}(\omega)G_4^{\nu\mu}(\omega) \left[\gamma_{1',4';1,3}^{\alpha\mu\gamma\eta}\gamma_{3',2';4,2}^{\rho\beta\nu\delta} + \gamma_{1',3';1,4}^{\alpha\rho\gamma\nu}\gamma_{4',2';3,2}^{\mu\beta\eta\delta} - \right. \\ &\quad \left. \left. \gamma_{2',4';1,3}^{\beta\mu\gamma\eta}\gamma_{3',1';4,2}^{\rho\alpha\nu\delta} - \gamma_{2',3';1,4}^{\beta\rho\gamma\nu}\gamma_{4',1';3,2}^{\mu\alpha\eta\delta} \right] \right) . \end{aligned} \quad (\text{B2})$$

Comparing (B2) with Eq. (20) in Ref. 38 we see that we have two more terms because of the Keldysh indices and in the first term $G^{\rho\eta}$, while its transpose $G^{\eta\rho}$ appears everywhere else.

Due to the necessary antisymmetry of γ_2 and spin conservation we can even further simplify expression (B2) by

introducing a new variable U defined by

$$\gamma_{1234}^{\alpha\beta\gamma\delta} = \delta_{1,3}\delta_{2,4}U^{\alpha\beta\gamma\delta} - \delta_{2,3}\delta_{1,4}U^{\beta\alpha\gamma\delta} ,$$

resulting in

$$\begin{aligned} \frac{\partial}{\partial\Lambda}U^{\alpha\beta\gamma\delta} &= \frac{1}{4\pi} \sum_{\omega=\pm\Lambda} \sum_{3,4} \sum_{\mu,\nu\rho,\eta} \left(G_3^{\rho\eta}(-\omega)G_4^{\nu\mu}(\omega) [U^{\alpha\beta\rho\nu}U^{\eta\mu\gamma\delta} + U^{\beta\alpha\rho\nu}U^{\mu\eta\gamma\delta}] - \right. \\ &\quad G_3^{\eta\rho}(\omega)G_4^{\nu\mu}(\omega) \left[2U^{\alpha\mu\gamma\eta}U^{\rho\beta\nu\delta} - U^{\alpha\mu\gamma\eta}U^{\beta\rho\nu\delta} - U^{\mu\alpha\gamma\eta}U^{\rho\beta\nu\delta} + \right. \\ &\quad 2U^{\alpha\rho\gamma\nu}U^{\mu\beta\eta\delta} - U^{\alpha\rho\gamma\nu}U^{\beta\mu\eta\delta} - U^{\rho\alpha\gamma\nu}U^{\mu\beta\eta\delta} - \\ &\quad \left. \left. U^{\mu\beta\gamma\eta}U^{\alpha\rho\nu\delta} - U^{\rho\beta\gamma\nu}U^{\alpha\mu\eta\delta} \right] \right) . \end{aligned} \quad (\text{B3})$$

From the initial value of γ_2 given in Eq. (38) we can read off as initial value for $U^{\alpha\beta\gamma\delta}$

$$\left[\begin{pmatrix} -iU & 0 \\ 0 & 0 \end{pmatrix} \quad \begin{pmatrix} \hat{0} \\ \begin{pmatrix} 0 & 0 \\ 0 & iU \end{pmatrix} \end{pmatrix} \right] .$$

¹ L. P. Keldysh, JETP **20**, 1018 (1965).

² A. Fetter and J. Walecka, *Quantum Theory of Many-Particle Systems*, International Series in Pure and Applied Physics (McGraw-Hill, New York, 1971).

³ U. Schollwöck, Rev. Mod. Phys. **77**, 259 (2005).

⁴ T. Costi, Phys. Rev. B **55**, 3003 (1997).

⁵ F. B. Anders and A. Schiller (2006), cond-mat/0604517.

⁶ D. Lobaskin and S. Kehrein, Phys. Rev. B **71**, 193303 (2005).

⁷ Y. Meir and N. S. Wingreen, Phys. Rev. Lett. **68**, 2512 (1992).

⁸ V. Koreemann, Ann. of Phys. **39**, 72 (1966).

⁹ D. Langreth, in *NATO advanced study institute Series B*, edited by J. Devreese and E. van Doren (Plenum New York/London, 1967), vol. 17.

¹⁰ B. Altshuler and Y. Aharonov, JETP **48**, 812 (1978).

¹¹ K. G. Wilson, Rev. Mod. Phys. **47**, 773 (1975).

¹² H. Schoeller, in *Low-Dimensional Systems*, edited by T. Brandes (Springer Verlag, 1999), vol. 17, p. 137.

¹³ H. Schoeller and J. König, Phys. Rev. Lett. **84**, 3686 (2000).

¹⁴ M. Keil and H. Schoeller, Phys. Rev. B **63**, 180302 (2001).

¹⁵ A. Rosch, J. Paaske, J. Kroha, and P. Wölfle, J. Phys. Soc. Jpn. **74**, 118 (2005).

¹⁶ F. Wegner, Ann. Physik (Leipzig) **3**, 77 (1994).

¹⁷ S. D. Glazek and P. B. Wiegmann, Phys. Rev. D **48**, 5863 (1993).

¹⁸ J. Polchinski, Nucl. Phys. B **231**, 269 (1984).

¹⁹ C. Wetterich, Phys. Lett. B **301**, 90 (1993).

²⁰ T. R. Morris, Int. J. Mod. Phys. A **9**, 2411 (1994).

²¹ M. Salmhofer, *Renormalization* (Springer, Berlin, 1998).

²² M. Salmhofer and C. Honerkamp, Prog. Theor. Phys. **105**, 1 (2001).

²³ R. Hedden, V. Meden, T. Pruschke, and K. Schönhammer, J. Phys.: Condens. Matter **16**, 5279 (2004).

²⁴ S. Jakobs, Diploma thesis, RWTH Aachen (2003).

²⁵ S. Jakobs, V. Meden, and H. Schoeller, in preparation.

²⁶ L. Canet, B. Delamotte, O. Deloubrière, and N. Wschebor, Phys. Rev. Lett. **92**, 195703 (2004).

²⁷ P. W. Anderson, Phys. Rev. **124**, 41 (1961).

²⁸ M. A. Kastner, Rev. Mod. Phys. **64**, 849 (1992).

²⁹ L. P. Kouwenhoven, D. G. Austing, and S. Tarucha, Rep. Prog. Phys. **64**, 701 (2001).

³⁰ J. Nygård, D. H. Cobden, and P. E. Lindelof, Nature **408**, 342 (2000).

³¹ V. Madhavan, W. Chen, T. Jamneala, M. F. Crommie, and N. S. Wingreen, Science **280**, 567 (1998).

³² J. Li, W.-D. Schneider, R. Berndt, and B. Delley, Phys. Rev. Lett. **80**, 2893 (1998).

³³ G. A. Fiete and E. J. Heller, Rev. Mod. Phys. **75**, 933 (2003).

³⁴ M. Pustilnik and L. Glazman, J. Phys.: Condens. Matter **16**, R513 (2004).

³⁵ A. Georges, G. Kotliar, W. Krauth, and M. J. Rozenberg, Rev. Mod. Phys. **68**, 13 (1996).

³⁶ T. Maier, M. Jarrell, T. Pruschke, and M. H. Hettler, Rev. Mod. Phys. **77**, 1027 (2005).

³⁷ S. Andergassen, T. Enss, and V. Meden, Phys. Rev. B **73**, 153308 (2006).

³⁸ C. Karrasch, T. Enss, and V. Meden, Phys. Rev. B **73**, 235337 (2006).

³⁹ L. Landau and E. Lifshitz, *Physical Kinetics* (Akademie-Verlag Berlin, 1983).

⁴⁰ J. Rammer and H. Smith, Rev. Mod. Phys. **58**, 323 (1986).

⁴¹ H. Haug and A.-P. Jauho, *Quantum Kinetics and Optics of Semiconductors* (Springer Verlag, 1996).

⁴² A. Kamenev, in *Les Houches, Volume Session LX*, edited by H. Bouchiat, Y. Gefen, S. Guéron, G. Montambaux, and J. Dalibard (Elsevier, North-Holland, 2004), cond-mat/0412296.

⁴³ J. Negele and H. Orland, *Quantum Many-Particle Physics* (Addison-Wesley, 1988).

⁴⁴ C. Honerkamp and M. Salmhofer, Phys. Rev. B **67**, 174504 (2003).

⁴⁵ A. Komnik and A. O. Gogolin, Phys. Rev. Lett. **94**, 216601 (2005).

⁴⁶ J. E. Han, Phys. Rev. B **73**, 125319 (2006).

⁴⁷ J. E. Han (2006), cond-mat/0604583.

⁴⁸ S. Hershfield, J. H. Davies, and J. W. Wilkins, Phys. Rev. Lett. **67**, 3720 (1991).

⁴⁹ S. Hershfield, J. H. Davies, and J. W. Wilkins, Phys. Rev. B **46**, 7046 (1992).

⁵⁰ Y. Meir, N. S. Wingreen, and P. A. Lee, Phys. Rev. Lett. **70**, 2601 (1993).

⁵¹ N. S. Wingreen and Y. Meir, Phys. Rev. B **49**, 11040 (1994).

⁵² T. Fujii and K. Ueda, Phys. Rev. B **68**, 155310 (2003).

⁵³ J. H. Han (2004), cond-mat/0405477.

⁵⁴ M. Hamaasaki (2005), cond-mat/0506752.

⁵⁵ S. Datta (2006), cond-mat/0603034.

⁵⁶ K. Thygesen and A. Rubio (2006), cond-mat/0609223.

⁵⁷ A. C. Hewson, *The Kondo Problem to Heavy Fermions*, Cambridge Studies in Magnetism (Cambridge University Press, Cambridge, 1993).

⁵⁸ L. P. Kouwenhoven et al., in *Mesoscopic Electron Transport*, edited by L. L. Sohn et al. (Dordrecht: Kluwer, 1997), p. 105.

⁵⁹ J. Takahashi and S. Tasaki (2006), cond-mat/0603337.